frontiers in Earth Science

ORIGINAL RESEARCH
published: 10 September 2021
doi: 10.3389/feart.2021.706144

Redox-Controlled Ammonium Storage and Overturn in Ediacaran Oceans

Christian Hallmann[1†], Emmanuelle Grosjean[1†], Nathan D. Shapiro[1†], Yuichiro Kashiyama[2,3], Yoshito Chikaraishi[2,4], David A. Fike[1†], Naohiko Ohkouchi[2] and Roger E. Summons[1]*

[1]Department of Earth, Atmospheric and Planetary Sciences, Massachusetts Institute of Technology, Cambridge, MA, United States, [2]Japan Agency for Marine-Earth Science and Technology, Yokosuka, Japan, [3]Graduate School of Engineering, Fukui University of Technology, Fukui, Japan, [4]ILTS, Hokkaido University, Sapporo, Japan

As a key nutrient, nitrogen can limit primary productivity and carbon cycle dynamics, but also evolutionary progress. Given strong redox-dependency of its molecular speciation, environmental conditions can control nitrogen localization and bioavailability. This particularly applies to periods in Earth history with strong and frequent redox fluctuations, such as the Neoproterozoic. We here report on chlorophyll-derived porphyrins and maleimides in Ediacaran sediments from Oman. Exceptionally light $\delta^{15}N$ values (< −10‰) in maleimides derived from anoxygenic phototrophs point towards ammonium assimilation at the chemocline, whereas the isotopic offset between kerogens and chlorophyll-derivatives indicates a variable regime of cyanobacterial and eukaryotic primary production in surface waters. Biomarker and maleimide mass balance considerations imply shallow euxinia during the terminal Ediacaran and a stronger contribution of anoxygenic phototrophs to primary productivity, possibly as a consequence of nutrient 'lockup' in a large anoxic ammonium reservoir. Synchronous $\delta^{13}C$ and $\delta^{15}N$ anomalies at the Ediacaran–Cambrian boundary may reflect one in a series of overturn events, mixing ammonium and isotopically-light DIC into oxic surface waters. By modulating access to nitrogen, environmental redox conditions may have periodically affected Ediacaran primary productivity, carbon cycle perturbations, and possibly played a role in the timing of the metazoan radiation across the terminal Ediacaran and early Cambrian.

Keywords: ediacaran, ammonium, porphyrin, nutrient, nitrogen, animal evolution

OPEN ACCESS

Edited by:
Eva Stüeken, University of St Andrews, United Kingdom

Reviewed by:
Michael Kipp, California Institute of Technology, United States
Carina Lee, Universities Space Research Association (USRA), United States

****Correspondence:***
Christian Hallmann
Christian.hallmann@gfz-potsdam.de

†Present address:
Christian Hallmann, GFZ, German Research Center for Geosciences, Potsdam, Germany
Emmanuelle Grosjean, Geoscience Australia, Canberra, ACT, Australia
Nathan D. Shapiro, Vir Biotechnology, Inc., San Francisco, CA, United States
David A. Fike, Department of Earth and Planetary Sciences, Washington University, Saint Louis, MO, United States

Specialty section:
This article was submitted to Geochemistry, a section of the journal Frontiers in Earth Science

Received: *06 May 2021*
Accepted: *25 August 2021*
Published: *10 September 2021*

Citation:
Hallmann C, Grosjean E, Shapiro ND, Kashiyama Y, Chikaraishi Y, Fike DA, Ohkouchi N and Summons RE (2021) Redox-Controlled Ammonium Storage and Overturn in Ediacaran Oceans. Front. Earth Sci. 9:706144. doi: 10.3389/feart.2021.706144

INTRODUCTION

An increase in algal diversity during the Ediacaran (Knoll et al., 2006) and the advent of metazoan organismic complexity (Love et al., 2009) have traditionally been attributed to enhanced oxygen availability (e.g., Catling et al., 2005) or the demise of widespread marine sulfidic conditions (e.g. Cohen et al., 2009) toxic to complex eukaryotes. But the realisation that basal metazoan metabolism can proceed under exceedingly low oxygen partial pressures (Mills et al., 2014), a limited spatial extent of pervasive euxinia (Reinhard et al., 2013) and a slow oxygenation that continued into the early Paleozoic (Sperling, 2015) warrant revisiting these hypotheses. Only recently have researchers begun to examine the role of marine redox conditions in controlling the abundance of essential nutrients that could have retarded or stimulated evolutionary processes. While an increase in bioavailable phosphorus likely fueled the rise of eukaryotic algae to ecological significance during the Cryogenian (Brocks et al., 2017), P/Fe ratios in iron formations (Planavsky et al., 2010), P in fine-

grained sediments (Reinhard et al., 2017) and an abundance of late Neoproterozoic peritidal phosphate deposits (Brasier, 1990) suggest that phosphorus was likely widely bioavailable in the Ediacaran ocean. In terms of understanding the role that bioavailable nitrogen has played during the later Neoproterozoic, most studies have focused on measuring bulk $\delta^{15}N$ values (e.g., Ader et al., 2014; Zhang et al., 2017; Wang et al., 2017; Wang et al., 2018a,b; Chen et al., 2019) yet there are limits to the amount of information that can be gained from bulk $\delta^{15}N$ signals. Here we aim to address this limitation by studying compound-specific $\delta^{15}N$ signals.

Repeated imbalance of the Neoproterozoic marine carbon cycle is evident from frequent and extreme stable carbon isotope fluctuations recorded in Ediacaran carbonates and kerogens (e.g., Halverson and Shields-Zhou, 2011), yet relatively little is known about Neoproterozoic nitrogen cycling (Ader et al., 2014) or its availability as a potentially limiting nutrient. In modern oceans, the carbon and nitrogen cycles are tightly coupled through biological dependence on the fixed inorganic nitrogen species nitrate (NO_3^-) and ammonium (NH_4^+), which frequently limit primary productivity (Falkowski and Godfrey, 2008). The primary source of these nutrients is the cyanobacterial fixation of dissolved N_2, but the subsequent fate and transformation of nitrogen species is strongly dependent on environmental redox conditions (Canfield et al., 2010), thereby implying a tight connection between ecosystem diversity, environmental conditions and biogeochemical cycling. In particular the Neoproterozoic Era witnessed strong water column redox gradients and temporal fluctuations thereof (Li et al., 2010; Sperling et al., 2013). This has been recorded by a notable instability in the secular stable carbon isotope curve (e.g., Halverson and Shields-Zhou, 2011), with many anomalies and excursions that may reflect chemocline instability (e.g., Jiang et al., 2008) on shorter time scales or oxidative events (Rothman et al., 2003). One of these, the largest recorded negative carbon isotope anomaly, can be traced globally (Grotzinger et al., 2011) and occurred during deposition of the Shuram Formation in the South Oman Salt Basin (Fike et al., 2006). During such redox-driven perturbations, the speciation of fixed nitrogen and the nitrogen cycle would have been vulnerable to environmental factors. Ediacaran redox variability could thus have indirectly exerted a significant control on nitrogen nutrient availability and the marine carbon cycle, as well as on ecosystem structure and evolution.

The stable nitrogen isotopic composition of sedimentary organic matter can be used to constrain the nitrogen source as well as isotopic fractionation during assimilation of the precursor biomass (Ohkouchi and Takano, 2014). However, the $\delta^{15}N$ value of bulk organic matter represents an amalgamated signal of primary producing bacteria and algae, as well as heterotrophs—all of which fractionate nitrogen isotopes differently during assimilation (Higgins et al., 2008). Nitrogen in sedimentary porphyrins that represent the diagenetic product of chlorophylls is not only covalently bound and resistant to diagenetic overprinting, but also highly source-specific (Sachs et al., 1999). Yet the sensitivity of porphyrins to geothermal heating precludes their survival in most Precambrian rocks that have experienced deep burial (Baker et al., 1987). The South Oman Salt Basin (SOSB; **Figure 1**) hosts one of the most complete and thermally best preserved Ediacaran sedimentary sequences (**Figure 2**; Fike et al., 2006; Amthor et al., 2003; Grosjean et al., 2009) that was initially deposited under open marine conditions (Nafun Group) and subsequently in a restricted but marine fed epicratonic basin (Ara Group), witnessing periodic transgressive cycles that led to the deposition of six (A0–A5) shallow water carbonate-evaporite couplets (Amthor et al., 2003; Mattes and Conway-Morris, 1990). These are well developed on the southern carbonate platform (**Figure 1**), with carbonate 'stringers' sandwiched between sulphate and halite evaporites, but form a more continuous carbonate platform on the eastern flank. For more details of the geology of the SOSB the reader is referred to (Gorin et al., 1982) or (Loosveld and Terken, 1996). An ash bed in the A4 unit of the Ara Group was U-Pb dated at 541 ± 0.13 Ma (Bowring et al., 2007) and contains a $\delta^{13}C_{carbonate}$ excursion that marks the Precambrian–Cambrian boundary. Rifting around 543 Ma opened up a deeper sub-basin (Athel Basin) that hosts organic rich fine siliciclastics of the U Shale and Thuleilat Fm, as well as the somewhat enigmatic Athel Silicilite, which all were deposited synchronously with the platform A4 carbonate-evaporite unit (**Figures 1**, **2**) and thus also record the Ediacaran–Cambrian boundary. The Athel Fm (or, Al Shomou silicilyte) is a thick, finely laminated and organic rich quartz deposit deposited in deep waters, which stands in marked contrast to other Neoproterozoic silica sinks that are largely restricted to peritidal settings (Stolper et al., 2017). However the carbonates of its laterally equivalent shallow water facies appear to lack authigenic chert (e.g., Schröder et al., 2005; Stolper et al., 2017). To date, the origin and uniqueness of this formation remain debated (Ramseyer et al., 2013; Al Rajaibi et al., 2015; Stolper et al., 2017). We here report on porphyrins and maleimides recovered from basinal Ediacaran sediments of the South Oman Salt Basin and discuss their stable nitrogen isotope values in the context of biological assimilation pathways and different nitrogen reservoirs in the Ediacaran ocean.

METHODS

Cutting aliquots weighing between ca. 3 and 20 g (**Supplementary Table S1**) were powdered in a stainless steel puck mill and solvent extracted with dichloromethane/methanol (DCM/MeOH, 9:1) in a Dionex Accelerated Solvent Extractor (ASE) device. Asphaltenes were precipitated from the resulting bitumen extracts using *n*-pentane. Asphaltene-free fractions were treated with activated copper in order to remove elemental sulfur and separated into saturated hydrocarbons, aromatic hydrocarbons and a polar fraction by open column liquid chromatography over silica gel, eluting sequentially with

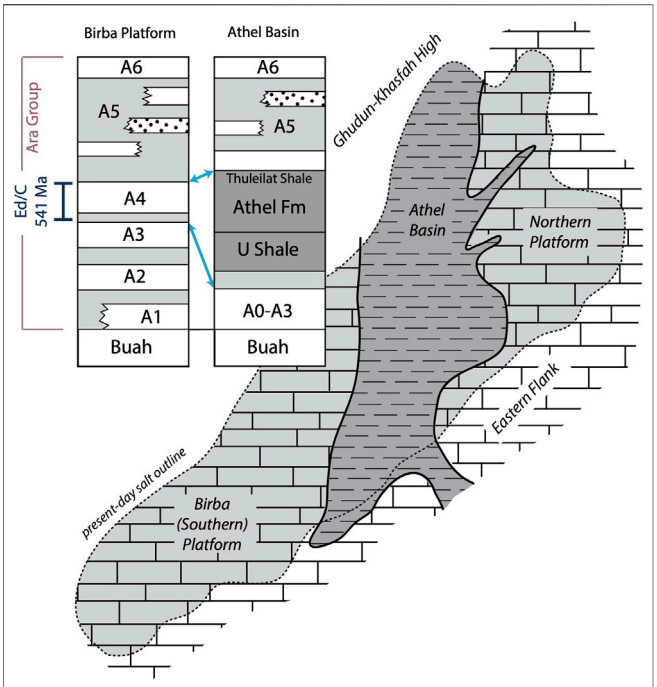

FIGURE 1 | Outline and stratigraphy of platform and basin in the South Oman Salt Basin. Deposits of the deep-water Athel subbasin are time equivalent to the A4 carbonate-evaporite couplet on the adjacent shallow platform. After Schröder et al. (2005).

n-hexane, *n*-hexane/DCM (1:1) and DCM/MeOH (1:1). The aromatic and polar fractions were further fractionated on a silica gel column to afford subfractions enriched in nickel and vanadyl porphyrins, respectively, by elution with DCM (Grice et al., 1996). Quantification of porphyrins was carried out on these enriched fractions using a UV-visible spectrophotometer as described in more detail elsewhere (Grosjean et al., 2004). While nickel porphyrins were not detected, vanadyl porphyrin concentrations were measured from visible spectra using an extinction coefficient of 31.6 L $mmol^{-1}$ cm^{-1} at 574 nm (Buchler et al., 1971; Mackenzie et al., 1981).

The porphyrin-enriched fractions were dissolved in DCM/MeOH (1:4 vol.) and analyzed on a Thermo Finnigan LCQ system fitted with a Hypersil BDS C_{18} column (4.6 × 150 mm) coupled to a UV photospectrometer and operated in full scan mode: *m/z* 400–1,500. During liquid chromatography samples were eluted at 0.8 ml/min with a concentration gradient from 100% MeOH (containing 0.1% formic acid) at t = 0–90% MeOH (containing 0.1% formic acid), 10% DCM at t = 15 min. Subsequently pure MeOH (containing 0.1% formic acid) was eluted for 10 further minutes.

A detailed procedure of the nitrogen isotope analysis of maleimides was described in (Chikaraishi et al., 2008) and is briefly described below. Porphyrin fractions were oxidized to maleimides using a 1:1 (v/v) mixture of 10% aqueous chromic acid and 15% aqueous H_2SO_4 at 0°C for 1 h and then at room temperature for 1 h (Nomoto et al., 2001). It was shown that this procedure involves no isotopic fractionation (Chikaraishi et al., 2008). Maleimides were extracted with benzene (5 x) from the solution. The extracts were then methyl-esterified and analyzed by GC-MS for screening. The nitrogen isotopic composition of maleimides was determined by GC-C-IRMS using an Agilent 6890N GC fitted with an Ultra-2 capillary column (25 m, 0.32 mm i.d., 0.52 μm film thickness) coupled to a Thermo Finnigan Delta Plus XP IRMS. The analytical error of repeated measurements was consistently better than 0.5‰. This number represents the average of analytical errors (1 sigma) of various in-house synthesized maleimide injections (also see Chikaraishi et al., 2008). The $\delta^{15}N$ values of these maleimides were independently determined at JAMSTEC on an EA/IRMS (described in Isaji et al., 2020) that was calibrated with IAEA authentic standards. Methyl-isobutyl-maleimides were below the limit of reliable analysis.

Bulk nitrogen isotope values shown in **Figure 2** ($\delta^{15}N_{org}$) and discussed in the context of the synchronicity of the $\delta^{13}C$ and $\delta^{15}N$ signals across the Ediacaran/Cambrian boundary derive from Chapter 4 in (Fike, 2007) and were determined at MIT on organic extracts (bitumens) in order to avoid falsification of the bulk organic $\delta^{15}N$ signal by nitrogen adsorbed on clay particles. Although likely to be offset from bulk $\delta^{15}N$ values, for samples of a similar range of moderate thermal maturity like the ones studied here, such offsets are likely small (Stueeken et al., 2017) and should not impact ensuing interpretations, especially if solely used to indicate stratigraphic trends (**Figure 2**). Bitumens were recovered by solvent extraction (dichloromethane/methanol 9:1 in a Dionex Accelerated Solvent Extractor), as described in (Fike, 2008), and the indigeneity of the bitumen was tested and asserted using biomarkers and stable isotope patterns. Bitumens were weighed into tin cups and flash combusted at 1,060°C in a Carlo Erba NA1500 Elemental Analyser fitted with an AS200 autosampler. The resulting gas, reduced to N_2 was analyzed in continuous flow mode using a Delta Plus XP Isotope Ratio Mass Spectrometer. Nitrogen isotope values are reported in units of per mil relative to Air after calibration using international standards and in-house references interspersed with the analysed samples (NBS-22, Acetanilide and Penn State kerogen).

Bulk $\delta^{15}N$ values shown in **Figure 5** and used for the calculation of ε values were determined at the Max-Planck-Institute for Biogeochemistry on kerogen isolates that were obtained after digestion of carbonates and silicates using aqueous HCl and HF, respectively. Despite an expected slight offset to whole-rock bulk $\delta^{15}N$ values, for the here studied unmetamorphosed rocks, both $\delta^{15}N_{kerogen}$ as well as $\delta^{15}N_{bulk}$ should be good approximations of $\delta^{15}N_{biomass}$ (Stueeken et al., 2017). Homogenized kerogen powders, weighed into tin cups, were flash combusted in an NA 1110 elemental analyser (CE Instruments) coupled to a Delta-Plus XL IRMS (Thermo Finnigan) *via* a ConFlow III. Nitrogen isotope values (averages of duplicate measurements) are reported in units of per mil relative to Air after calibration using in-house reference standards acetanilide ($\delta^{15}N$ = −1.51 ± 0.1 permit and caffeine ($\delta^{15}N$ = −15.46 ± 0.1 per mil). For further details of this method see (Werner and Brand, 2001).

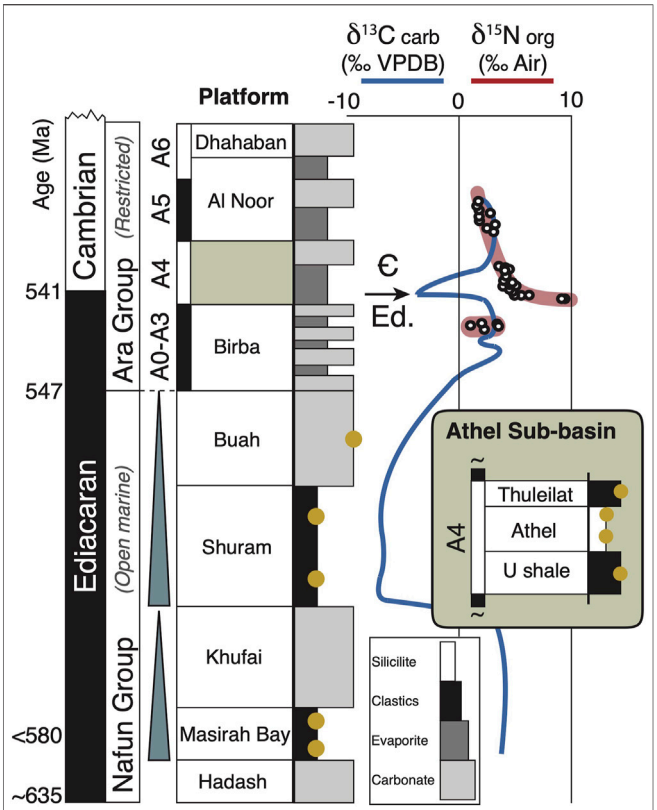

FIGURE 2 | Composite stratigraphy and stable isotope record of the South Oman Salt Basin. Studied samples (yellow circles) represent both open marine and more restricted basinal depositional environments. A composite stable carbon isotope curve (based on platform carbonates [after: Amthor et al., 2003] shows the Shuram anomaly and a characteristic excursion at the Ediacaran–Cambrian boundary. A precisely coincident positive nitrogen isotope anomaly first reported by Fike (2007) suggests a causal connectivity, interpreted as the consequence of sudden overturn and oxidation of a large deep-water pool of ammonium into shallow oxygenated surface waters. Shaded box shows deep-water equivalent strata to the A4 platform carbonates.

RESULTS AND DISCUSSION

Intact Preserved Neoproterozoic Porphyrins

LC-UVvis and LC-MS revealed the presence of intact porphyrin molecules in 18 of the 27 studied samples, with only vanadyl-complexed species and both DPEP (deoxophylloerythroetioporphyrins) and Etio (etioporphyrins) structures being present (**Figure 3**), which are characterised by a closed or opened pentacyclic ring, respectively. Given the conversion of DPEP to Etio during thermal maturation (Baker et al., 1987), we conclude that the observed VO-porphyrin dominance throughout the Ediacaran SOSB sedimentary sequence (**Table 1**) is not due to thermal destruction of the generally more labile Ni-porphyrins (Baker et al., 1987) but rather points to environmental conditions: sulfidic bottom waters in the SOSB may have periodically removed any available nickel by precipitation as insoluble sulfides (Lewan, 1984) and left an excess of vanadium to react with labile organic matter. On the basis of observed concentrations, only VO-chelates underwent detailed characterization as intact porphyrins. These revealed the highest concentrations of up to ~16 nmol/g rock in the youngest stratigraphic units that experienced the least burial (**Figure 4**), while porphyrin abundances decrease systematically with overall greater burial depth of older stratigraphic levels (**Figure 5**). Given a concomitant increase in hopanoid biomarker maturation parameters (based on 'Ts': 18α–22,29,30-trisnorneohopane and 'Tm': 17α–22,29,30-trisnorhopane), this decrease can be directly linked to progressive thermal destruction during sedimentary burial in the South Oman Salt Basin (**Figure 6A**). Oddly, silicilyte rocks of the Athel Formation are characterized by a paucity of porphyrins despite a suitable thermal maturation window (**Figures 5**, **6A**). The enigmatic nature and source of the Athel silica is subject to ongoing debate (e.g., Al Rajaibi et al., 2015; Stolper et al., 2017) and these results may suggest that the relative proportion of phototrophically derived organic matter in this stratigraphic unit was exceedingly small, thereby supporting the possibility of silica precipitation by nucleation on elevated levels of dissolved organic matter as a consequence of strongly enhanced heterotrophy (Ferris et al., 1988).

The detection of a wide range of VO-porphyrins, including structures > C_{33}, in all of the other stratigraphic units indicates an original input of both chlorophyll-a (*Chl-a*) and bacteriochlorophylls (*BChl*), including such structures adapted to light intensities at greater water depths and typically biosynthesized by anoxygenic phototrophs inhabiting chemoclines. To allow for their stable isotopic analyses, whole porphyrin fractions were oxidized to GC-amenable maleimides in the laboratory (**Figure 2**). This process involves no isotopic fractionation (Chikaraishi et al., 2008) and the retention of characteristic alkylation patterns allows for the recognition of precursor-product relationships. Structural and isotopic studies have previously shown that maleimides with a methyl-ethyl substitution pattern (MEM) are principally derived from *Chl-a* and thus largely representative of carbon and nitrogen fixation in surface waters, whereas both methyl-n-propyl (MPM) and methyl-isobutyl maleimides (MBM) largely derive from the same (Naeher et al., 2013) Chlorobi-derived *BChl-c*, *BChl-d* or *BChl-e* molecular precursors (Grice et al., 1996) that are indicative of processes occurring in anoxic waters below a chemocline.

Nitrogen Isotopes and Nutrient Assimilation in Surface Waters: Cyanobacteria and Algae

By knowing the stable nitrogen isotopic fractionation that occurs during porphyrin biosynthesis, the original composition of precursor biomass ($\delta^{15}N_{biomass}$) can be reconstructed from $\delta^{15}N_{porphyrin}$. By now several studies have focused on this biosynthetic fractionation ($\varepsilon_{por} = \delta^{15}N_{biomass}–\delta^{15}N_{porphyrn}$) and found that eukaryotic algae typically fractionate by 5–7‰ (Kennicutt et al., 1992; Sachs, 1997; Sachs et al., 1999; Sachs and Repeta, 1999; Sigman et al., 2009; Higgins et al., 2011) meaning that the pigments are depleted in ^{15}N relative to biomass. Negative epsilon values of freshwater cyanobacteria

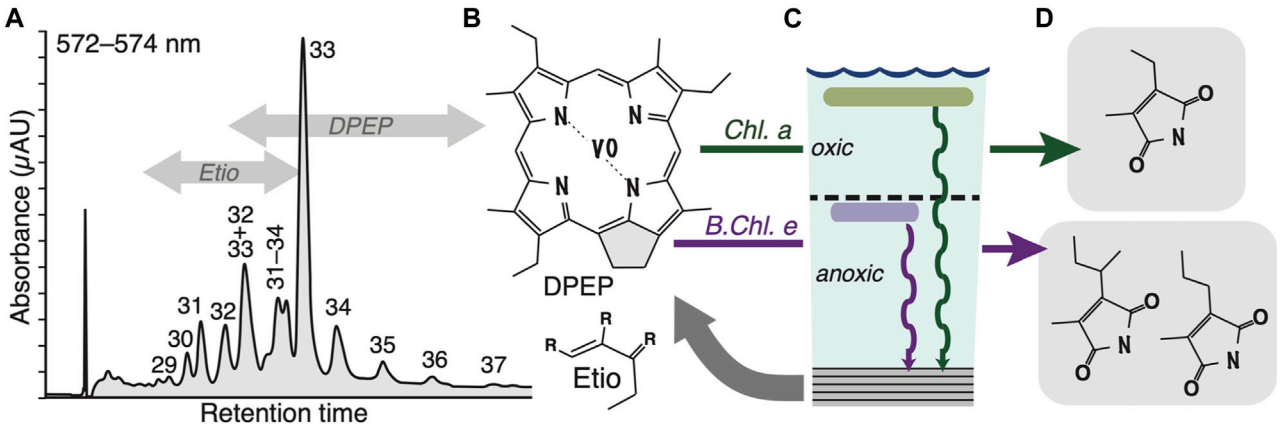

FIGURE 3 | Porphyrins and maleimides. Intact vanadyl porphyrins in SOSB sediments were characterized by LC-MS and quantified by UV*vis* spectrophotometry **(A,B)**. Chromatographic peaks in (a.) (sample OMR-11, Thuleilat Fm) are annotated by their corresponding carbon numbers. Porphyrins > C_{32} indicate the presence of both chlorophyll-a and bacteriochlorophyll-derived structures that were biosynthesized in surface waters and at the chemocline, respectively **(C)**. Oxidation to maleimides **(D)** does not affect the characteristic alkylation pattern, allowing the distinction of maleimides primarily deriving from surface water chlorophyll-a (MEM) versus structures deriving from bacteriochlorophyll-c, -d or-e (MPM, MBM), produced by anoxygenic phototrophs.

TABLE 1 | Organic carbon, hopanoid-derived thermal maturity (Ts and Tm) and normalized porphyrin concentrations in studied samples.

Unit	Sample	Depth min (m)	Depth max (m)	TOC (wt%)	Ts/(Ts + Tm)	Porphyrins (nmol/g rock)	(nmol/g TOC)
Masirah Bay	OMR027	2,280	2,295	3.8	0.25	0.0	0.0
Masirah Bay	OMR009	2,648	2,676	4.4	0.41	0.7	16.8
Masirah Bay	OMR015	2026	2060	4.7	0.31	0.8	17.7
Masirah Bay	OMR016	3,177	3,196	1.7	0.53	0.0	0.0
Shuram	OMR008	2,380	2,500	2.5	0.45	1.8	70.3
Shuram	OMR010	2,628	2,724	2.5	0.46	0.0	0.0
Shuram	OMR018	1,486	1,518	4.1	0.31	2.4	57.7
Shuram	OMR019	930	990	3.7	0.35	1.1	29.6
Shuram	OMR026	1905	1940	3.4	0.18	1.9	57.2
Shuram	OMR001	2,440	2,460	2.3	0.41	1.6	69.5
Buah	OMR002	2,344	2,374	1.6	0.31	4.5	281.5
Buah	OMR017	1,569	1,602	2.3	0.26	2.9	126.5
Buah	OMR020	4,411	_	3.1	0.53	0.0	0.0
U Shale	OMR005	1,425	1,527	3.5	0.21	10.1	288.4
U Shale	OMR006	1,527	1,650	4.9	0.16	9.9	202.5
U Shale	OMR007	1773	1872	5.7	0.27	8.4	146.8
U Shale	OMR014	2,420	2,460	6.4	0.34	4.7	74.0
U Shale	OMR025	1751	1833	4.0	0.3	3.3	82.5
Silicilyte	OMR004	1,198	1,425	3.4	0.22	0.0	0.0
Silicilyte	OMR013	2,240	2,352	2.3	0.21	0.0	0.0
Silicilyte	OMR024	1,628	1742	2.6	0.26	0.0	0.0
Silicilyte	OMR012	2,104	2,120	3.4	0.18	0.0	0.0
Silicilyte	OMR023	1,551	1,602	4.3	0.28	0.0	0.0
Thuleilat	OMR003	1,000	1,102	8.0	0.23	16.0	200.4
Thuleilat	OMR011	2068	2084	10.4	0.21	7.6	73.3
Thuleilat	OMR021	1,417.5	1,483	6.4	0.25	12.6	197.5
Thuleilat	OMR022	1,520	1,547	2.5	0.28	2.3	91.5

(Higgins et al., 2011; i.e. porphyrins heavier than biomass by ~10‰) are irrelevant to this study given that a marine depositional environment is well constrained for the studied deposits, whereas marine cyanobacteria tend to be characterized by exceedingly low ε_{por} values around 0‰ (Higgins et al., 2011). The variability of ε_{por} values appears to be independent of phylogeny (Higgins et al., 2011) and, because ε_{por} reflects intracellular partitioning of N isotopes downstream of glutamate, it is also independent of N substrate (Higgins et al., 2011, 2012). In the marine realm *Chl-a*, which is the principal molecular precursor to MEM, is predominantly biosynthesized by eukaryotic algae and cyanobacteria. Hence, when reconstructing $\delta^{15}N_{biomass}$ from $\delta^{15}N_{porphyrin}$ values we must consider both end-member options.

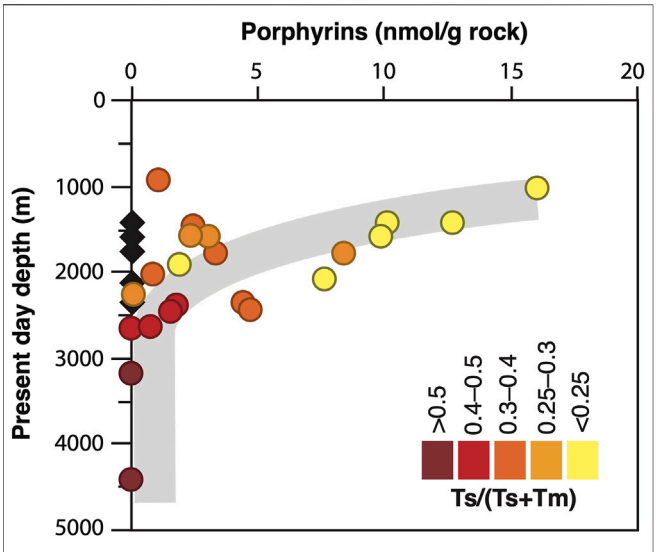

FIGURE 4 | Porphyrin preservation. Relationship between present-day burial depth of studied samples, their thermal maturity (*via* the hopanoids Ts and Tm) and porphyrin content. Overall, the porphyrin content decreases with increasing burial and thermal maturity, which corresponds to the stratigraphic trend shown in **Figure 5A**. Despite some variation, the oldest stratigraphic units have mostly also experienced the greatest burial (see **Table 1**). Black diamonds indicate samples from the Athel silicilyte, which contain no porphyrins despite a low thermal maturity (0.18–0.28 on the Ts/(Ts + Tm) scale).

In the studied SOSB samples, surface water derived MEM that principally reflect *Chl-a* exhibit $\delta^{15}N$ values ranging between −5.2‰ and +7.2‰ (Air) (**Figure 5**). If these maleimides were derived 100% from cyanobacteria, an identical range of values could be reconstructed for the bulk precursor biomass. Given an average $\delta^{15}N$ value of + 0.7‰ for dissolved marine N_2 and the fact that the nitrogenase enzyme typically fractionates by 0–2‰ ($\varepsilon_{assimilation}$, Higgins et al., 2011; Bauersachs et al., 2009), the biomass of diazotrophic marine cyanobacteria should carry average values around −1.3‰ (Higgins et al., 2011) and should not be lighter than −2‰ (Higgins et al., 2012). This implies that the lighter range of observed MEM values (i.e., those between −5.2‰ and ca. −2.0‰) cannot be attributed to nitrogen fixing cyanobacteria utilising the common and widespread Mo-based nitrogenase enzyme. These ^{15}N-depleted values may reflect the cyanobacterial use of a different substrate, a (partial) eukaryotic source of MEM or the activity of 'alternative' (i.e., Fe- or V-based) nitrogenases. The latter may have been more active under Mo-scarce conditions, as possibly induced by strong euxinia, and fractionate more strongly during nitrogen fixation, leading to lower $\delta^{15}N$ values (Zhang et al., 2014). Under the assumed environmental conditions, which will be discussed in more detail further below, such alternative nitrogenases could indeed have been relevant. However the role that such alternative nitrogenases have generally played in the geological past is unknown and debated, and it remains unresolved when they evolved (Boyd et al., 2011; Garcia et al., 2020). As will also be discussed in more detail further below, we consider the cyanobacterial use of different substrates—nitrate or, more likely, ammonium—as the most plausible source of the observed light isotopic values. Despite typically higher positive environmental $\delta^{15}N_{nitrate}$ values that are a consequence of microbial water-column denitrification (Sigman et al., 2009), a stronger fractionation during assimilation can generate cyanobacterial $\delta^{15}N_{biomass}$ values as light as −5.3‰ (corresponding to $\varepsilon_{assimilation}$ of 10.2‰, Higgins et al., 2012). Alternatively, cyanobacterial assimilation of ammonium may be considered, which can explain $\delta^{15}N_{biomass} < 2.0$ and lead to values as low as −5.0‰ ($\varepsilon_{assimilation}$ of 13.9‰) in Anabaena (Macko et al., 1987). In principle, the full range of $\delta^{15}N_{MEM}$ can plausibly be explained by a sole cyanobacterial source of primary produced organic matter in surface waters of the SOSB. Nevertheless, the studied deposits are not low in eukaryotic steranes, indicating that algae did provide a contribution to fossilized biomass.

Assuming a 100% contribution of eukaryotic algae to MEM, on the other hand, the precursor biomass can be reconstructed to $\delta^{15}N$ values between −0.2 and 12.2‰ (ε_{por} = ~5 ± 2‰, Sachs et al., 1999; Higgins et al., 2011). The heavier range of these values would be typical for nitrate-assimilating eukaryotic algae and zooplankton (e.g., Minagawa and Wada, 1984; Sigman et al., 2009) but these processes are incompatible with observed values around 0‰. Here again, the lighter range of values can be achieved when algae assimilate ammonium ($\varepsilon_{assimilation}$ of −6.7‰ to +7.2‰; average −0.92 ± 3.88‰; data from Table 1 in Higgins et al., 2011). Taking into account that we need to find an explanation for $\delta^{15}N_{MEM}$ between −5.2‰ and ca. −2.0‰ that likely cannot be attributed to diazotrophic cyanobacteria or to nitrate-assimilating algae, it appears likely that ammonium may have played a relevant role as a nitrogen substrate for Ediacaran primary producers, as will be discussed in more detail below.

Apart from allowing for the tentative reconstruction of the main nitrogen substrates used during assimilation, the wide range of observed values likely suggests that surface waters were inhabited by a mixed population of diazotrophic cyanobacteria, nitrate- or ammonium-assimilating cyanobacteria and eukaryotic algae. This is corroborated by ε_{por} values (kerogen–MEM)—i.e. $\Delta\delta^{15}N_{kerogen-MEM}$ that can yield further insight to the source of biomass under the assumption that $\delta^{15}N_{biomass} \approx {}^{15}N_{kerogen}$. In organic-rich sediments, such as the here-studied SOSB rocks (with total organic carbon [TOC] values between 1.6 and 10.4%: **Table 1**), $\delta^{15}N_{kerogen}$ is considered to faithfully reflect $\delta^{15}N_{biomass}$ (Robinson et al., 2012). The SOSB rocks (early-middle oil window) have never seen the advanced stages of thermal maturation during which $\delta^{15}N_{kerogen}$ values are significantly altered (Boudou et al., 2008). With the previously discussed knowledge—and under exclusion of freshwater cyanobacteria—the ε_{por} values can be used to tentatively differentiate between marine cyanobacterial and marine algal primary production (Higgins et al., 2011, 2012). The $\Delta\delta^{15}N_{kerogen-MEM}$ values obtained on SOSB samples range from −3.82 to +8.79 (**Figure 5**; **Table 2**), where the higher values are most likely characteristic of eukaryote-dominated primary productivity in surface waters (Higgins et al., 2011). This is not surprising, since a rise of mostly green algae (Hoshino et al., 2017) to ecological dominance was recorded at the onset of

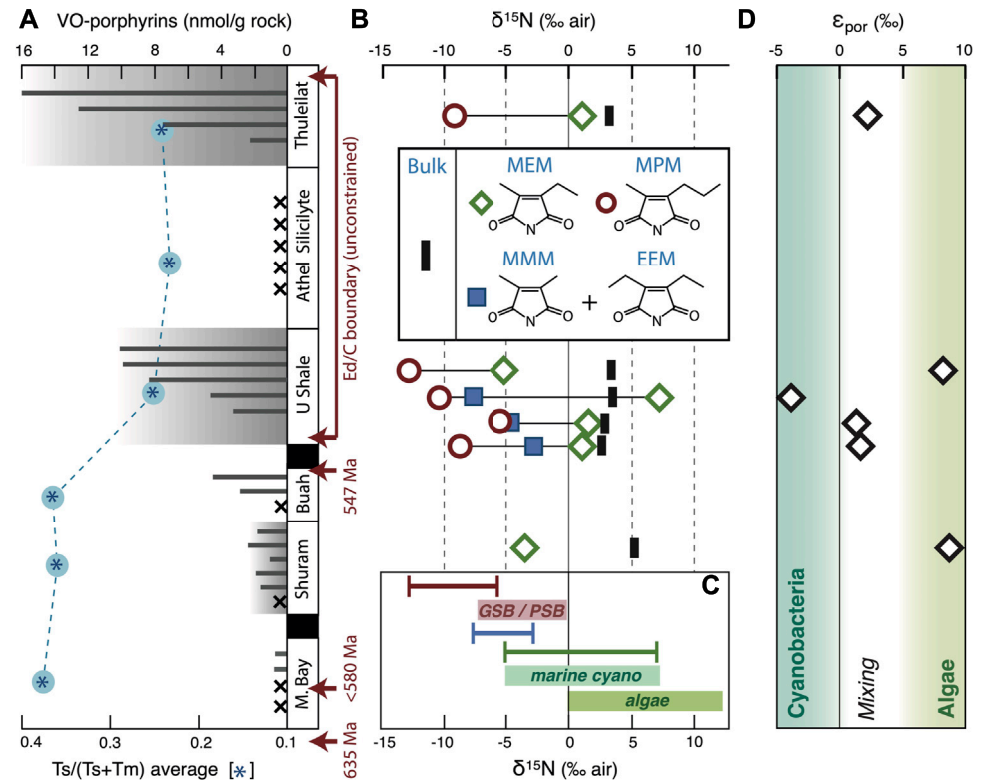

FIGURE 5 | Porphyrin abundances and maleimide nitrogen isotopes. **(A)** VO-porphyrin abundances (grey bars; plotted per stratigraphic unit irrespective of exact depth) decrease with burial and thermal maturity (blue asterisks; based on the hopanoids Ts and Tm: **Figure 6**). Crosses indicate absent porphyrins. **(B)** $\delta^{15}N$ values of kerogens and maleimides were determined for six samples only due to concentration and matrix interference. **(C)** Ranges of observed values (colored lines) and $\delta^{15}N_{biomass}$ values converted from $\delta^{15}N_{maleimide}$ based on known biosynthetic fractionation during porphyrin biosynthesis after Higgins et al., 2011 (annotated boxes) place constraints on nitrogen substrate and assimilatory processes. **(D)** The kerogen–MEM isotopic offset allows reconstructing the dominant primary producers (Higgins et al., 2011, 2012).

the Ediacaran (Brocks et al., 2017; van Maldegem et al., 2019) and C_{27}–C_{29} steranes are prominently present in all studied SOSB samples (Grosjean et al., 2009). The negative ε_{por} values observed in some samples, however imply primary productivity that is strongly shifted towards marine cyanobacteria (Higgins et al., 2011). While overall algae dominated marine productivity during the Ediacaran, the range of $\Delta\delta^{15}N_{kerogen-MEM}$ values observed here suggests that fluctuations in the composition of the primary producing community occurred during the course of the Ediacaran with periodic return to (cyano)bacterial dominance. In broad terms, this is in agreement with a strikingly large variation of bacterial hopanes over eukaryotic steranes observed throughout the Ediacaran (Brocks et al., 2017; Pehr et al., 2018; van Maldegem et al., 2019), which led to the suggestion that on regional scales primary productivity was likely modulated by local determinants such as nutrient supply (Pehr et al., 2018). It is also consistent with distributions of carotenoid pigments (Cui et al., 2020).

Nitrogen Isotopes and Nutrients at the Chemocline: Ammonium Assimilation

In contrast to MEM, deriving from cyanobacterial or algal *Chl-a* in surface waters, MPM is thought to largely derive from anoxygenic phototrophs thriving at a deeper chemocline. In contrast to MBM, which can *only* derive from anoxygenic phototrophs, but whose abundances were too low to allow for the reliable determination of $\delta^{15}N$ values in the here studied samples, MPM can theoretically represent a mixture of anoxygenic phototroph-derived MPM and an additional MPM-component deriving from *Chl*-a by phytyl ester hydrolysis and reduction of the resulting C-3 acid (Baker et al., 1987; Verne-Mismer et al., 1986). In principle, the relative contribution of anoxygenic phototrophs engaging in the rTCA cycle for carbon fixation to the pool of fossil MPM can be recognized on the basis of 'heavy' $\delta^{13}C$ values. Yet this was not achieved in the present study due to chromatographic co-elution: although we managed to purify the samples sufficiently to allow for the chromatographic baseline separation of individual maleimides from other nitrogen-bearing compounds, we could not achieve a baseline separation from other carbon-containing molecules. Nevertheless, in practical terms MPM and MBM seem to largely derive from the same biological precursors, which has been confirmed in multiple individual instances where MBM and MPM concentrations are linearly correlated with R^2 values of 0.95–0.99 (Naeher et al., 2013, 2015), confirming that these compounds either share the same origin or that populations of source bacteria thrive under the same, highly specific

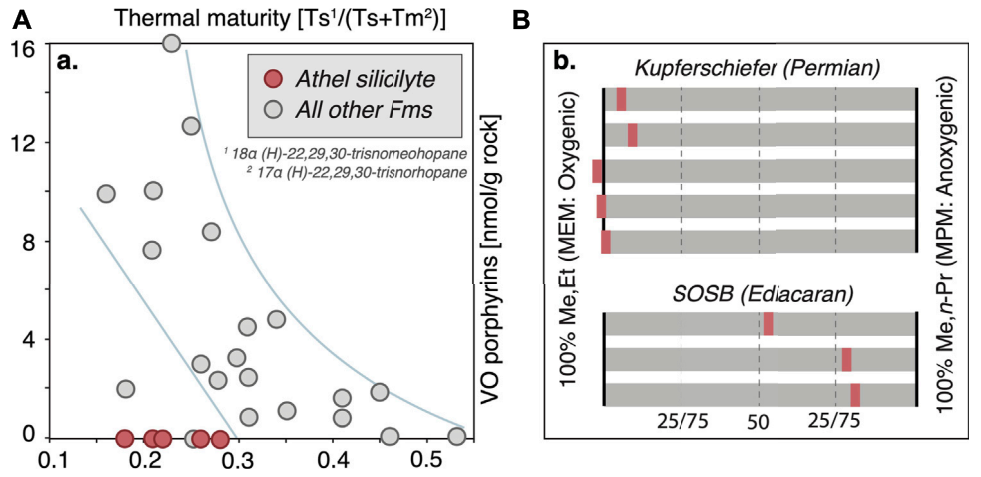

FIGURE 6 | Preservation of porphyrins and mass balance of autotrophy. **(A)** Porphyrin abundances are a function of preservation and thermal maturity (based on the hopanoids Ts and Tm; see main text). VO-porphyrins are systematically absent from the Athel Fm (red symbols) despite a suitable thermal maturity, pointing to strongly differing ecologies or environmental conditions. **(B)** Isotopic mass balance calculations (^{13}C for the Kupferschiefer after Grice et al., 1997: **Supplementary Table S3**; ^{15}N for the SOSB: **Table 2**) on the basis of comparing the isotope value of summed MMM and EEM to those of MEM and MPM end members can hint towards the relative proportion of oxygenic vs anoxygenic phototrophic biomass. SOSB primary productivity during deposition of the U-shale ($n = 3$) was shifted towards a markedly higher contribution of anoxygenic phototrophs. Negative values for some Kupferschiefer samples, i.e. $\delta^{13}C_{MMM+EEM}$ beyond the 0–100% spectrum spanned by $\delta^{13}C_{MEM}$ and $\delta^{13}C_{MPM}$, likely derive from analytical error.

TABLE 2 | Stable nitrogen isotopic composition of kerogen and maleimides in studied samples.

Unit	Sample	Depth min (m)	Depth max (m)	$\delta^{15}N$ (ker)	$\delta^{15}N$ maleimides (‰ air)			ε por (Ker–MEM)
					MEM	MPM	MMM + EEM	
U Shale	OMR006	1,527	1,650	2.7	1.1	–8.8	–2.8	1.6
U Shale	OMR007	1773	1872	2.8	1.5	–5.1	–5.0	1.3
U Shale	OMR014	2,420	2,460	3.4	7.2	–10.5	–7.7	–3.8
Thuleilat	OMR021	1,417.5	1,483	3.2	1.0	–9.3	n.a	2.2
U Shale	OMR025	1751	1833	3.1	-5.2	–13.0	n.a	8.3
Shuram	OMR026	1905	1940	5.20	-3.6	n.a	n.a	8.8

environmental conditions (Naeher et al., 2013). In samples of the Permian Kupferschiefer, (Grice et al., 1997), found MPM to be isotopically similar to MBM: with a simple mixing model of two samples characterized by $\delta^{13}C_{MBM}$ of –15.4‰ and –14.7‰, $\delta^{13}C_{MPM}$ of –17.0‰ and –17.3‰ and $\delta^{13}C_{MEM}$ of –26.2‰ and –25.9‰ (data from Table 3 and from Figure 8 in Grice et al., 1997) we can reconstruct that not more than 14.8–23.2% of all MPM in the Kupferschiefer samples (Grice et al., 1997) derives from a different biological source, implying that MPM sufficiently faithfully represents anoxygenic phototrophs.

Characterized by $\delta^{15}N$ values of –5.1‰ to –13.0‰, MPM in the here studied SOSB samples, largely reflecting nitrogen assimilation at the chemocline, carry some of the lightest biological stable nitrogen isotope values ever reported (**Figure 5**). These numbers systematically exclude either diazotrophy, which is rare in anoxygenic phototrophs (Madigan, 1995), or the assimilation of nitrate. Some cyanobacteria assimilating ammonium are known to fractionate strongly ($\varepsilon_{assimilation}$ of 13.9‰, Macko et al., 1987) but cyanobacteria tend to produce significantly more MEM than MPM and rarely generate $\delta^{15}N_{biomass}$ <–5‰ (*nota bene* that alternative nitrogenases may generate $\delta^{15}N_{biomass}$ as low as –7 or –8‰; Zhang et al., 2014), and hence even lighter porphyrins. Unfortunately, our knowledge of nitrogen isotope fractionation during assimilation and porphyrin biosynthesis by anoxygenic phototrophs is highly limited. As a best approximation, it has been shown that *Rhodobacter capsulatus*, a purple non-sulfur bacterium, fractionates by 0.8–1.8‰ ($\varepsilon_{assimilation}$) during photoautotrophic and photoheterotrophic growth on N_2, whereas these values increase to 10.6 and 12.4‰ during photoheterotrophic growth with NH_4^+ (Beaumont et al., 2000). Porphyrins synthesized during growth on ammonium were depleted relative to biomass (ε_{por}) by another 8.6–10.9‰, leading to *BChl-a* as light as –21.0‰ (Beaumont et al., 2000) despite much heavier biomass. Hence the presence of this process would never be visible in bulk $\delta^{15}N$ values of fossil organic matter. We conclude that the most likely explanation for observed light $\delta^{15}N_{MPM}$ values in the SOSB lies in a scenario involving assimilation of ammonium (Higgins et al., 2011, 2012; Vo et al., 2013) that likely accumulated in deep anoxic waters,

similar to what is frequently observed in modern stratified meromictic lakes such as Lake Cadagno and Lake Kaiike (e.g,. Ohkouchi et al., 2005, 2007; Halm et al., 2009). Although not providing a direct analog in terms of salinity and the presence of benthic phototrophic mats that were likely absent in deeper facies of the SOSB, stratified Lake Kaiike contains relevant amounts of dissolved ammonium below a chemocline inhabited by green and purple sulfur bacteria, whose *BChl-e* is characterized by similarly low $\delta^{15}N$ values to those found in the SOSB (Ohkouchi et al., 2005, 2007). At present, such a scenario provides the most plausible explanation for the anomalously light nitrogen isotopes encountered in MPM of the studied SOSB samples.

Isotope Mass Balance Suggests Significant Anoxygenic Productivity

Me, Me- and Et, Et-maleimides (MMM, EEM) are considered as source-unspecific since they can potentially derive from both *Chl-a* and from *BChls*. In modern, predominantly aerobic marine ecosystems, the relative proportion of anoxygenic phototrophs dwindles in comparison to oxygenic primary producers (Raven, 2009), which is evident from the molecular sedimentary remnants of phototrophic organisms: bacteriochlorophyll-derived porphyrins and farnesane are much less common than *Chl-a* derived porphyrins and phytyl hydrocarbons. Since independent of the nitrogen substrate used, MMM and EEM represent a mixture between a purely anoxygenic phototrophic source on one hand (*BChl*) and a mostly oxygenic phototrophic source (*Chl-a*) on the other, their stable isotopic composition—be it nitrogen *or* carbon—in comparison to those of MEM and MPM, can be used to establish a rough mass balance of phototrophic primary productivity.

Under modern aerobic conditions, the $\delta^{15}N$ value of MMM + EEM should lie close to that of MEM, given dominant oxygenic photosynthesis in surface waters, and such a constellation of values is even observed during episodes of mild euxinia (**Figure 6**), when reconstructing the predominant source of MMM and EEM using their $\delta^{13}C$ values in samples of the Permian Kupferschiefer (using data from Grice et al., 1997). Results from the SOSB that are based on $\delta^{15}N$ suggest that MMM and EEM are isotopically much more similar to MPM. Given the uncommon light $\delta^{15}N$ values of MPM that we attribute to chemocline-dwelling phototrophs, we posit that a significant portion of MMM and EEM is predominantly derived from *BChls* biosynthesized at the chemocline, and hence from anoxygenic phototrophs (**Figure 6B**). This appears to contradict the relatively low abundance of VO-porphyrins > C_{33} (**Figure 3**), but it must be kept in mind that the fate of *Chls* after demetallation is highly complex and that many different, yet uncharacterized chelates can form that evade characterization (Gueneli et al., 2018). Even if MPM do not constitute a pure anoxygenic phototrophic end member but contain some non-*BChl* sourced portion (e.g., up to ca. 25% as calculated for the Kupferschiefer), the SOSB ecosystem would still be remarkably different from modern oceans in that a sizable portion of productivity was performed by anoxygenic phototrophs in deeper waters. Considering the possibility of a preservational bias, a larger proportion of *Chl-a* produced in surface waters may indeed be oxidatively degraded than *BChl* produced at the chemocline, thereby artificially shifting the balance of preserved porphyrins towards anoxygenic phototrophs. However, episodic euxinia with a shallow chemocline was corroborated for deep-water facies of the SOSB by the presence of the molecular markers okenane and chlorobactane (French et al., 2015; Roussel et al., 2020). In the deep-water depositional environments of the SOSB, the observed carotenoid pigments cannot derive from benthic mats but must represent planktonic purple sulfur bacteria and the green strains of green sulfur bacteria, respectively—microbes requiring access to reduced sulfur and with high light requirements. In the absence of isorenieratane that derives from brown strains of green sulfur bacteria, and irrespective of the generally lesser ecological relevance of green sulfur bacteria prior to the Phanerozoic (Cui et al., 2020), these data point to persistent stratification and a shallow chemocline (<25 m, Brocks and Schaeffer, 2008). Given the short transit through oxygenated surface waters, any preferential degradation of surface-derived *Chl* may have been minimal. From this perspective the reconstructed mass balance would not require significant correction to account for preservational biases. On the other hand one could argue that remineralisation rates tend to be highest in the upper water column, where organic export fluxes are highest, whereas the maintenance of euxinic conditions requires a particularly high remineralisation rate in shallow waters in order to maintain anoxia. From this perspective a relevant preservation bias may be given. Nevertheless if such biases were large, they should have similarly affected the Kupferschiefer samples that are not shifted towards an anoxygenic phototrophic source of MMM and EEM despite only mild euxinia (Grice et al., 1997). Most recently, a study of fossil aromatic carotenoids in terminal Ediacaran SOSB sediments (Roussel et al., 2020) reported an elevated proportion of structures that were likely sourced by cyanobacteria rather than by anoxygenic phototrophs (Cui et al., 2020). However, the taphonomy of carotenoids is complicated by sulfide as a preferential preservative (e.g., Koopmans et al., 1996) and although we cannot exclude principally-cyanobacterial productivity in the SOSB, it is unlikely that ^{15}N-depleted MMM, EEM and *BChl*-derived MPM were all largely produced by cyanobacteria. Hence despite the paucity of comparative data, and accepting that we may face some degree of preservation bias, we posit that during the terminal Ediacaran a relevant portion of photosynthetic primary production in the distal facies of the SOSB (Athel subbasin) could have been taking place at the chemocline and not in surface waters.

While such conditions do not exist in modern oceans, the best modern analogue environments are shallow stratified lakes, where anoxygenic phototrophs can indeed dominate primary production (van Gemenden and Mas, 1995), and which are known to develop an ammonium reservoir in deeper anoxic waters (Ohkouchi et al., 2005). In trying to understand the here presented data, we hypothesize on a model where under persistently stratified conditions, sinking biomass of marine primary producers continuously contributed nitrogen to a deep-water ammonium pool in the SOSB, whose diffusion back up into the mixed zone would have been minimal. This

large pool of reduced nitrogen remained inaccessible to aerobic primary producers inhabiting surface waters. With an exceedingly shallow chemocline, suggested by the biomarkers okenane and chlorobactene, the biomass of diazotrophic cyanobacteria containing freshly fixed nitrogen would have rapidly exited the mixed layer, maintaining nitrogen scarcity in surface waters. This in turn would have led to a relative shift in overall primary productivity towards anoxygenic phototrophs inhabiting the chemocline and tapping into the deep pool of reduced nitrogen. In this scenario, the deep-water ammonium that is controlled by the redox structure of the water column represents a 'locked-up' nutrient reservoir capable of modulating primary productivity: under persistently stratified conditions, primary productivity will be throttled, whereas the overturn of such a setting will release abundant nutrients and stimulate surface water productivity.

Periodic Ammonium Overturn and Nutrient Release

The Ediacaran–Cambrian boundary in the SOSB not only records a characteristic and well-documented negative $\delta^{13}C_{CARB}$ anomaly (Halverson and Shields-Zhou, 2011; Fike et al., 2006; Amthor et al., 2003) but (Fike, 2007) also reported a positive $\delta^{15}N_{ORG}$ excursion with an exactly synchronous onset, which jumps abruptly from values around 1–3‰ to values close to 10‰ before gradually returning to pre-excursion values (**Figure 2**). Apart from the perfect synchronicity of their onset, nitrogen and carbon isotopes are not directly correlated (**Supplementary Table S2**), thereby rather excluding an explanation by coupled ammonium oxidation and methanotrophy (Thomazo et al., 2011). Rather than intense denitrification and depletion of the nitrate reservoir, as seen in modern low-productivity ocean regions (Sigman et al., 2009), we suggest that these heavy nitrogen isotopes may be the result of intense nitrate assimilation, which discriminates against ^{15}N with ~5‰, caused by enhanced productivity following basinal overturn and oxidation of a deep ammonium reservoir. Alternatively, direct cyanobacterial utilization of liberated ammonium—sourced from upwelling or overturn—could result in similar heavy values, as a consequence of Rayleigh fractionation of ammonium during anoxygenic photosynthetic assimilation. Such a situation was observed in meromictic Lake Kaiike (Ohkouchi et al., 2005) and may also provide an explanation for heavy MEM values (**Figure 5**). In the first scenario, availability of NO_3^- supplied by nitrification is eventually dependent on oxidant and NH_4^+ availability. Given persistent oxic surface waters as testified by the $\delta^{15}N$ of MEM and overall elevated ε_{por}, we suggest that Ediacaran surface water productivity could have been episodically limited by deep-water nutrient capture during stratified sulfidic conditions, and stimulated by overturn—the observed anomalies at the Ediacaran–Cambrian boundary (**Figure 1**) representing one such overturn event. Strong environmental redox fluctuations (e.g., Sperling et al., 2013; Li et al., 2010) could have exerted principal control on nitrogen nutrient availability by controlling the N supply pathway, thereby modulating primary productivity on shorter time scales and providing an explanation for the repeated return to cyanobacterial-dominated (Pehr et al., 2018) and mixed ecosystems (**Figure 5D**) during the Ediacaran. Models have suggested that the Ediacaran transition towards an oxygen-rich ocean-atmosphere system was inhibited or delayed by a need for elevated abundances of fixed nitrogen (Reinhard et al., 2017). The here suggested mechanistic link to redox-driven nitrogen nutrient dynamics may not only solve the timing of the latter, but also provides an explanation for the aberrant Neoproterozoic carbon cycle, while the progressive overturn of 'locked-up' nitrogen around the Ediacaran-Cambrian boundary could have contributed towards the enhanced nutrient requirements of an increasingly complex biosphere.

CONCLUSION

Together with previously published accounts of fossil pigments (French et al., 2015; Roussel et al., 2020), the distribution and stable nitrogen isotope composition of vanadyl porphyrins and porphyrin-derived maleimides in sediments of the Ediacaran SOSB is indicative of shallow euxinia. The $\delta^{15}N$ values of surface water (*Chl-a*) derived maleimides likely indicates the presence of both cyanobacteria as well as eukaryotic algae, as confirmed by steroid abundances in SOSB rocks (Grosjean et al., 2009), yet ranges into values that may point towards the use of ammonium as a nitrogen substrate. This notion is strengthened by $\delta^{15}N$ of chemocline (*BChl*) derived maleimides, whose exceptionally light values are best explained by the assimilation of ammonium by anoxygenic phototrophs (Beaumont et al., 2000; Vo et al., 2013), in analogy to the situation in some stratified meromictic lakes (Ohkouchi et al., 2005, 2007). Notably, such information would remain masked by bulk $\delta^{15}N$ analyses only. In such modern lake systems, a sizable portion of primary productivity can be shifted towards anoxygenic phototrophs. Using an isotope mass balance of maleimides we reconstruct a similar ecosystem structure for the SOSB and tentatively attribute this currently rare condition to the redox-controlled storage of ammonium-nitrogen in deep waters, which may have been periodically overturned. A coupled negative $\delta^{13}C$ and positive $\delta^{15}N$ excursion at the Ediacaran–Cambrian boundary (Fike, 2007) may reflect one such overturn event that released ^{13}C-depleted DIC and ammonium into surface waters, where it would be rapidly oxidized to nitrate and subjected to denitrification and algal assimilation. Our data may be explained by redox-controlled nitrogen scarceness in surface waters, which would have restricted eukaryotic, and reduced cyanobacterial activity. Under such conditions access to fixed nitrogen would have exerted fundamental control on phytoplankton community structure and possibly primary productivity (Johnston et al., 2009). Although more investigation is needed, such redox-driven nitrogen limitation may have played a role in delaying the transition to a fully oxygenated atmosphere-ocean system (Reinhard et al., 2017) and possibly the timing for the rise of animals.

DATA AVAILABILITY STATEMENT

The original contributions presented in the study are included in the article/**Supplementary Material**, further inquiries can be directed to the corresponding author.

AUTHOR CONTRIBUTIONS

EG, NO, DF, NS, YK, YC, and RS performed research and analyzed data; CH analyzed and interpreted data and wrote the paper with input from all others.

ACKNOWLEDGMENTS

Samples for this study were provided by Shell International E & P. Petroleum Development Oman provided financial support for the early stages of this work. Additional MIT research was supported by the NASA Astrobiology Institute NNA13AA90A Foundations of Complex Life. CH thanks the Agouron Institute for support. NO was financially supported by grants from JSPS. Petroleum Development Oman and the Oman Ministry of Oil and Gas are thanked for the permission to publish.

SUPPLEMENTARY MATERIAL

The Supplementary Material for this article can be found online at: https://www.frontiersin.org/articles/10.3389/feart.2021.706144/full#supplementary-material

REFERENCES

Ader, M., Sansjofre, P., Halverson, G. P., Busigny, V., Trindade, R. I. F., Kunzmann, M., et al. (2014). Ocean Redox Structure across the Late Neoproterozoic Oxygenation Event: a Nitrogen Isotope Perspective. *Earth Planet. Sci. Lett.* 396, 1–13. doi:10.1016/j.epsl.2014.03.042

Al Rajaibi, I. M., Hollis, C., and Macquaker, J. H. (2015). Origin and Variability of a Terminal Proterozoic Primary Silica Precipitate, Athel Silicilyte, South Oman Salt Basin, Sultanate of Oman. *Sedimentology* 62, 793–825. doi:10.1111/sed.12173

Amthor, J. E., Grotzinger, J. P., Schröder, S., Bowring, S. A., Ramezani, J., Martin, M. W., et al. (2003). Extinction of Cloudina and Namacalathus at the Precambrian-Cambrian Boundary in Oman. *Geol* 31, 431–434. doi:10.1130/0091-7613(2003)031<0431:eocana>2.0.co;2

Baker, E. W., William Louda, J., and Orr, W. L. (1987). Application of Metalloporphyrin Biomarkers as Petroleum Maturity Indicators: The Importance of Quantitation. *Org. Geochem.* 11, 303–309. doi:10.1016/0146-6380(87)90041-6

Bauersachs, T., Schouten, S., Compaoré, J., Wollenzien, U., Stal, L. J., and Sinninghe Damsteé, J. S. (2009). Nitrogen Isotopic Fractionation Associated with Growth on Dinitrogen Gas and Nitrate by Cyanobacteria. *Limnol. Oceanogr.* 54, 1403–1411. doi:10.4319/lo.2009.54.4.1403

Beaumont, V. I., Jahnke, L. L., and des Marais, D. J. (2000). Nitrogen Isotopic Fractionation in the Synthesis of Photosynthetic Pigments in Rhodobacter Capsulatus and Anabaena Cylindrica. *Org. Geochem.* 31, 1075–1085. doi:10.1016/s0146-6380(00)00133-9

Boudou, J.-P., Schimmelmann, A., Ader, M., Mastalerz, M., Sebilo, M., and Gengembre, L. (2008). Organic Nitrogen Chemistry during Low-Grade Metamorphism. *Geochimica et Cosmochimica Acta* 72, 1199–1221. doi:10.1016/j.gca.2007.12.004

Bowring, S. A., Grotzinger, J. P., Condon, D. J., Ramezani, J., Newall, M. J., Phillip, A., et al. (2007). Geochronological Constraints on the Chronostratigraphic Framework of the Neoproterozoic Huqf Supergroup, Sultanate of Oman. *Am. J. Sci.* 307, 1097–1145. doi:10.2475/10.2007.01

Boyd, E. S., Hamilton, T. L., and Peters, J. W. (2011). An Alternative Path for the Evolution of Biological Nitrogen Fixation. *Front. Microbio.* 2, 205. doi:10.3389/fmicb.2011.00205

Brasier, M. D. (1990). "Phosphogenic Events and Skeletal Preservation across the Precambrian-Cambrian Boundary Interval,". *Phosphorite Research and Development*. Editors A. J. G. Notholt and I. Jarvis (London: Geological society special publication), 52, 289–303. doi:10.1144/gsl.sp.1990.052.01.21

Brocks, J. J., Jarrett, A. J. M., Sirantoine, E., Hallmann, C., Hoshino, Y., and Liyanage, T. (2017). The Rise of Algae in Cryogenian Oceans and the Emergence of Animals. *Nature* 548, 578–581. doi:10.1038/nature23457

Brocks, J. J., and Schaeffer, P. (2008). Okenane, a Biomarker for Purple Sulfur Bacteria (Chromatiaceae), and Other New Carotenoid Derivatives from the 1640Ma Barney Creek Formation. *Geochimica et Cosmochimica Acta* 72, 1396–1414. doi:10.1016/j.gca.2007.12.006

Buchler, J. W., Eikelmann, G., Puppe, L., Rohbock, K., Schneehage, H. H., and Weck, D. (1971). Metallkomplexe mit Tetrapyrrol-Liganden, III. Darstellung von Metallkomplexen des Octaäthylporphins aus Metall-acetylacetonaten. *Justus Liebigs Ann. Chem.* 745, 135–151. doi:10.1002/jlac.19717450117

Canfield, D. E., Glazer, A. N., and Falkowski, P. G. (2010). The Evolution and Future of Earth's Nitrogen Cycle. *Science* 330, 192–196. doi:10.1126/science.1186120

Catling, D. C., Glein, C. R., Zahnle, K. J., and McKay, C. P. (2005). Why O2Is Required by Complex Life on Habitable Planets and the Concept of Planetary "Oxygenation Time". *Astrobiology* 5, 415–438. doi:10.1089/ast.2005.5.415

Chen, Y., Diamond, C. W., Stüeken, E. E., Cai, C., Gill, B. C., Zhang, F., et al. (2019). Coupled Evolution of Nitrogen Cycling and Redoxcline Dynamics on the Yangtze Block across the Ediacaran-Cambrian Transition. *Geochimica et Cosmochimica Acta* 257, 243–265. doi:10.1016/j.gca.2019.05.017

Chikaraishi, Y., Kashiyama, Y., Ogawa, N. O., Kitazato, H., Satoh, M., Nomoto, S., et al. (2008). A Compound-specific Isotope Method for Measuring the Stable Nitrogen Isotopic Composition of Tetrapyrroles. *Org. Geochem.* 39, 510–520. doi:10.1016/j.orggeochem.2007.08.010

Cohen, P. A., Knoll, A. H., and Kodner, R. B. (2009). Large Spinose Microfossils in Ediacaran Rocks as Resting Stages of Early Animals. *Proc. Natl. Acad. Sci.* 106, 6519–6524. doi:10.1073/pnas.0902322106

Cui, X., Liu, X.-L., Shen, G., Ma, J., Husain, F., Rocher, D., et al. (2020). Niche Expansion for Phototrophic Sulfur Bacteria at the Proterozoic-Phanerozoic Transition. *Proc. Natl. Acad. Sci. USA* 117, 17599–17606. doi:10.1073/pnas.2006379117

Falkowski, P. G., and Godfrey, L. V. (2008). Electrons, Life and the Evolution of Earth's Oxygen Cycle. *Phil. Trans. R. Soc. B* 363, 2705–2716. doi:10.1098/rstb.2008.0054

Ferris, F. G., Fyfe, W. S., and Beveridge, T. J. (1988). Metallic Ion Binding by Bacillus Subtilis: Implications for the Fossilization of Microorganisms. *Geol* 16, 149–152. doi:10.1130/0091-7613(1988)016<0149:mibbbs>2.3.co;2

Fike, D. A., Grotzinger, J. P., Pratt, L. M., and Summons, R. E. (2006). Oxidation of the Ediacaran Ocean. *Nature* 444, 744–747. doi:10.1038/nature05345

Fike, D. (2007). Carbon and Sulfur Isotopic Constraints on Ediacaran Biogeochemical Processes, Huqf Supergroup, Sultanate of Oman. PhD thesis. Cambridge, MA: Massachusetts Institute of Technology, 232.

French, K. L., Rocher, D., Zumberge, J. E., and Summons, R. E. (2015). Assessing the Distribution of Sedimentary C40carotenoids through Time. *Geobiology* 13, 139–151. doi:10.1111/gbi.12126

Garcia, A. K., McShea, H., Kolaczkowski, B., and Kaçar, B. (2020). Reconstructing the Evolutionary History of Nitrogenases: Evidence for Ancestral Molybdenum-Cofactor Utilization. *Geobiology* 18, 394–411. doi:10.1111/gbi.12381

Gorin, G. E., Racz, L. G., and Walter, M. R. (1982). Late Precambrian–Cambrian Sediments of the Huqf Group, Sultanate of Oman. *Am. Assoc. Pet. Geologists Bull.* 66, 2609–2627. doi:10.1306/03b5ac82-16d1-11d7-8645000102c1865d

Grice, K., Gibbison, R., Atkinson, J. E., Schwark, L., Eckardt, C. B., and Maxwell, J. R. (1996). Maleimides (1H-Pyrrole-2,5-Diones) as Molecular Indicators of Anoxygenic Photosynthesis in Ancient Water Columns. *Geochimica et Cosmochimica Acta* 60, 3913–3924. doi:10.1016/0016-7037(96)00199-8

Grice, K., Schaeffer, P., Schwark, L., and Maxwell, J. R. (1997). Changes in Palaeoenvironmental Conditions during Deposition of the Permian Kupferschiefer (Lower Rhine Basin, Northwest Germany) Inferred from Molecular and Isotopic Compositions of Biomarker Components. *Org. Geochem.* 26, 677–690. doi:10.1016/s0146-6380(97)00036-3

Grosjean, E., Adam, P., Connan, J., and Albrecht, P. (2004). Effects of Weathering on Nickel and Vanadyl Porphyrins of a Lower Toarcian Shale of the Paris Basin. *Geochimica et Cosmochimica Acta* 68, 789–804. doi:10.1016/s0016-7037(03)00496-4

Grosjean, E., Love, G. D., Stalvies, C., Fike, D. A., and Summons, R. E. (2009). Origin of Petroleum in the Neoproterozoic-Cambrian South Oman Salt Basin. *Org. Geochem.* 40, 87–110. doi:10.1016/j.orggeochem.2008.09.011

Grotzinger, J. P., Fike, D. A., and Fischer, W. W. (2011). Enigmatic Origin of the Largest-Known Carbon Isotope Excursion in Earth's History. *Nat. Geosci* 4, 285–292. doi:10.1038/ngeo1138

Gueneli, N., McKenna, A. M., Ohkouchi, N., Boreham, C. J., Beghin, J., Javaux, E. J., et al. (2018). 1.1-billion-year-old Porphyrins Establish a marine Ecosystem Dominated by Bacterial Primary Producers. *Proc. Natl. Acad. Sci. USA* 115, E6978–E6986. doi:10.1073/pnas.1803866115

Halm, H., Musat, N., Lam, P., Langlois, R., Musat, F., Peduzzi, S., et al. (2009). Co-occurrence of Denitrification and Nitrogen Fixation in a Meromictic lake, Lake Cadagno (Switzerland). *Environ. Microbiol.* 11, 1945–1958. doi:10.1111/j.1462-2920.2009.01917.x

Halverson, G. P., and Shields-Zhou, G. (2011). Chapter 4 Chemostratigraphy and the Neoproterozoic Glaciations. *Geol. Soc. Lond. Mem.* 36, 51–66. doi:10.1144/m36.4

Higgins, M. B., Robinson, R. S., Casciotti, K. L., McIlvin, M. R., and Pearson, A. (2008). A Method for Determining the Nitrogen Isotopic Composition of Porphyrins. *Anal. Chem.* 81, 184–192. doi:10.1021/ac8017185

Higgins, M. B., Robinson, R. S., Husson, J. M., Carter, S. J., and Pearson, A. (2012). Dominant Eukaryotic export Production during Ocean Anoxic Events Reflects the Importance of Recycled NH4+. *Proc. Natl. Acad. Sci.* 109, 2269–2274. doi:10.1073/pnas.1104313109

Higgins, M. B., Wolfe-Simon, F., Robinson, R. S., Qin, Y., Saito, M. A., and Pearson, A. (2011). Paleoenvironmental Implications of Taxonomic Variation Among δ15N Values of Chloropigments. *Geochimica et Cosmochimica Acta* 75, 7351–7363. doi:10.1016/j.gca.2011.04.024

Hoshino, Y., Poshibaeva, A., Meredith, W., Snape, C., Poshibaev, V., Versteegh, G. J. M., et al. (2017). Cryogenian Evolution of Stigmasteroid Biosynthesis. *Sci. Adv.* 3, e1700887. doi:10.1126/sciadv.1700887

Isaji, Y., Ogawa, N. O., Boreham, C. J., Kashiyama, Y., and Ohkouchi, N. (2020). Evaluation of δ13C and δ15N Uncertainties Associated with the Compound-specific Isotope Analysis of Geoporphyrins. *Anal. Chem.* 92, 3152–3160. doi:10.1021/acs.analchem.9b04843

Jiang, G., Zhang, S., Shi, X., and Wang, X. (2008). Chemocline Instability and Isotope Variations of the Ediacaran Doushantuo basin in South China. *Sci. China Ser. D-earth Sci.* 51, 1560–1569. doi:10.1007/s11430-008-0116-2

Johnston, D. T., Wolfe-Simon, F., Pearson, A., and Knoll, A. H. (2009). Anoxygenic Photosynthesis Modulated Proterozoic Oxygen and Sustained Earth's Middle Age. *Proc. Natl. Acad. Sci.* 106, 16925–16929. doi:10.1073/pnas.0909248106

Kennicutt, M. C., Bidigare, R. R., Macko, S. A., and Keeney-Kennicutt, W. L. (1992). The Stable Isotopic Composition of Photosynthetic Pigments and Related Biochemicals. *Chem. Geology. Isotope Geosci. section* 101, 235–245. doi:10.1016/0009-2541(92)90005-p

Knoll, A. H., Javaux, E. J., Hewitt, D., and Cohen, P. (2006). Eukaryotic Organisms in Proterozoic Oceans. *Phil. Trans. R. Soc. B* 361, 1023–1038. doi:10.1098/rstb.2006.1843

Koopmans, M. P., Köster, J., Van Kaam-Peters, H. M. E., Kenig, F., Schouten, S., Hartgers, W. A., et al. (1996). Diagenetic and Catagenetic Products of Isorenieratene: Molecular Indicators for Photic Zone Anoxia. *Geochimica et Cosmochimica Acta* 60, 4467–4496. doi:10.1016/s0016-7037(96)00238-4

Lewan, M. D. (1984). Factors Controlling the Proportionality of Vanadium to Nickel in Crude Oils. *Geochimica et Cosmochimica Acta* 48, 2231–2238. doi:10.1016/0016-7037(84)90219-9

Li, C., Love, G. D., Lyons, T. W., Fike, D. A., Sessions, A. L., and Chu, X. (2010). A Stratified Redox Model for the Ediacaran Ocean. *Science* 328, 80–83. doi:10.1126/science.1182369

LoosveldBell, R. A., and Terken, J. (1996). The Tectonic Evolution of interior Oman. *GeoArabia* 1, 28–51.

Love, G. D., Grosjean, E., Stalvies, C., Fike, D. A., Grotzinger, J. P., Bradley, A. S., et al. (2009). Fossil Steroids Record the Appearance of Demospongiae during the Cryogenian Period. *Nature* 457, 718–721. doi:10.1038/nature07673

Mackenzie, A. S., Patience, R. L., and Maxwell, J. R. (1981). "Molecular Changes and the Maturation of Sedimentary Organic Matter," in Proceedings of the Third Annual Karcher Symposium, Oklahoma, May 4 1979. Editors G. Atkinson and J. J. Zuckerman (Elsevier). doi:10.1016/b978-0-08-026179-9.50005-0

Macko, S. A., Fogel, M. L., Hare, P. E., and Hoering, T. C. (1987). Isotopic Fractionation of Nitrogen and Carbon in the Synthesis of Amino Acids by Microorganisms. *Chem. Geology. Isotope Geosci. section* 65, 79–92. doi:10.1016/0168-9622(87)90064-9

Madigan, M. T. (1995). "Microbiology of Nitrogen Fixation by Anoxygenic Photosynthetic Bacteria," in *Advances in Photosynthesis and Respiration. Anoxygenic Photosynthetic Bacteria*. Editors R. E. Blankenship, M. T. Madigan, and C. E. Bauer (Springer), Vol. 2, 915–928 .

Mattes, B. W., and Conway Morris, S. (1990). "Carbonate/evaporite Deposition in the Late Precambrian - Early Cambrian Ara Formation of Southern Oman,". *The Geology and Tectonics of the Oman Region*. Editor A. H. F. Robertson (London: Geological Society [London] Special Publication), 49, 617–636. doi:10.1144/gsl.sp.1992.049.01.37

Mills, D. B., Ward, L. M., Jones, C., Sweeten, B., Forth, M., Treusch, A. H., et al. (2014). Oxygen Requirements of the Earliest Animals. *Proc. Natl. Acad. Sci.* 111, 4168–4172. doi:10.1073/pnas.1400547111

Minagawa, M., and Wada, E. (1984). Stepwise Enrichment of 15N along Food Chains: Further Evidence and the Relation between δ15N and Animal Age. *Geochimica et Cosmochimica Acta* 48, 1135–1140. doi:10.1016/0016-7037(84)90204-7

Naeher, S., and Grice, K. (2015). Novel 1 H -Pyrrole-2,5-Dione (Maleimide) Proxies for the Assessment of Photic Zone Euxinia. *Chem. Geology.* 404, 100–109. doi:10.1016/j.chemgeo.2015.03.020

Naeher, S., Schaeffer, P., Adam, P., and Schubert, C. J. (2013). Maleimides in Recent Sediments - Using Chlorophyll Degradation Products for Palaeoenvironmental Reconstructions. *Geochimica et Cosmochimica Acta* 119, 248–263. doi:10.1016/j.gca.2013.06.004

Nomoto, S., Kozono, M., Mita, H., and Shimoyama, A. (2001). Structural Elucidation of an Oxidation Product of Sedimentary Porphyrins by One-Pot Synthesis of 3-methylphthalimide. *Bcsj* 74, 1975–1976. doi:10.1246/bcsj.74.1975

Ohkouchi, N., Nakajima, Y., Ogawa, N. O., and Chikaraishi, Y. (2007). Carbon Isotopic Composition of the Tetrapyrrole Nucleus in Chloropigments from a saline Meromictic lake: A Mechanistic View for Interpreting the Isotopic Signature of Alkyl Porphyrins in Geological Samples *Org. Geochem* 39, 521–531 .

Ohkouchi, N., Nakajima, Y., Okada, H., Ogawa, N. O., Suga, H., Oguri, K., et al. (2005). Biogeochemical Processes in the saline Meromictic Lake Kaiike, Japan: Implications from Molecular Isotopic Evidences of Photosynthetic Pigments. *Environ. Microbiol.* 7, 1009–1016. doi:10.1111/j.1462-2920.2005.00772.x

Ohkouchi, N., and Takano, Y. (2014). "Organic Nitrogen: Sources, Fates, and Chemistry," in *Treatise on Geochemistry. Organic Geochemistry*. Editors P. Falkowski and K. Freeman. second edition, 12, 251–289. doi:10.1016/b978-0-08-095975-7.01015-9

Pehr, K., Love, G. D., Kuznetsov, A., Podkovyrov, V., Junium, C. K., Shumlyanskyy, L., et al. (2018). Ediacara Biota Flourished in Oligotrophic and Bacterially Dominated marine Environments across Baltica. *Nat. Commun.* 9, 1807. doi:10.1038/s41467-018-04195-8

Planavsky, N. J., Rouxel, O. J., Bekker, A., Lalonde, S. V., Konhauser, K. O., Reinhard, C. T., et al. (2010). The Evolution of the marine Phosphate Reservoir. *Nature* 467, 1088–1090. doi:10.1038/nature09485

Ramseyer, K., Amthor, J. E., Matter, A., Pettke, T., Wille, M., and Fallick, A. E. (2013). Primary Silica Precipitate at the Precambrian/Cambrian Boundary in the South Oman Salt basin, Sultanate of Oman. *Mar. Pet. Geology.* 39, 187–197. doi:10.1016/j.marpetgeo.2012.08.006

Raven, J. (2009). Contributions of Anoxygenic and Oxygenic Phototrophy and Chemolithotrophy to Carbon and Oxygen Fluxes in Aquatic Environments. *Aquat. Microb. Ecol.* 56, 177–192. doi:10.3354/ame01315

Reinhard, C. T., Planavsky, N. J., Gill, B. C., Ozaki, K., Robbins, L. J., Lyons, T. W., et al. (2017). Evolution of the Global Phosphorus Cycle. *Nature* 541, 386–389. doi:10.1038/nature20772

Reinhard, C. T., Planavsky, N. J., Robbins, L. J., Partin, C. A., Gill, B. C., Lalonde, S. V., et al. (2013). Proterozoic Ocean Redox and Biogeochemical Stasis. *Proc. Natl. Acad. Sci.* 110, 5357–5362. doi:10.1073/pnas.1208622110

Robinson, R. S., Kienast, M., Albuquerque, A. L., Altabet, M., Contreras, S., Dubois, N., et al. (2012). A Review of Nitrogen Isotopic Alteration in marine Sediments. *Paleoceanography* 27, PA4203. doi:10.1029/2012pa002321

Rothman, D. H., Hayes, J. M., and Summons, R. E. (2003). Dynamics of the Neoproterozoic Carbon Cycle. *Pnas* 100, 8124–8129. doi:10.1073/pnas.0832439100

Roussel, A., Cui, X., and Summons, R. E. (2020). Biomarker Stratigraphy in the Athel Trough of the South Oman Salt Basin at the Ediacaran Cambrian Boundary. *Geobiology* 18, 663–681. doi:10.1111/gbi.12407

Sachs, J. P. (1997). Nitrogen Isotope Ratios in Chlorophyll and the Origin of Eastern Mediterranean Sapropels. Ph.D. Thesis. Cambridge, MA: Massachusetts Institute of Technology/Woods Hole Oceanographic Institute.

Sachs, J. P., Repeta, D. J., and Goericke, R. (1999). Nitrogen and Carbon Isotopic Ratios of Chlorophyll from marine Phytoplankton. *Geochimica et Cosmochimica Acta* 63, 1431–1441. doi:10.1016/s0016-7037(99)00097-6

Sachs, J. P., and Repeta, D. J. (1999). Oligotrophy and Nitrogen Fixation during Eastern Mediterranean Sapropel Events. *Science* 286, 2485–2488. doi:10.1126/science.286.5449.2485

Schröder, S., Grotzinger, J. P., Amthor, J. E., and Matter, A. (2005). Carbonate Deposition and Hydrocarbon Reservoir Development at the Precambrian-Cambrian Boundary: The Ara Group in South Oman. *Sediment. Geology.* 180, 1–28. doi:10.1016/j.sedgeo.2005.07.002

Sigman, D. M., Karsh, K. L., and Casciotti, K. L. (2009). "Nitrogen Isotopes in the Ocean," in *Encyclopedia of Ocean Sciences*. Editors J. H. Steele, S. A. Thorpe, and K. K. Turekian (Oxford: Academic Press), 40–54. doi:10.1016/b978-012374473-9.00632-9

Sperling, E. A., Halverson, G. P., Knoll, A. H., Macdonald, F. A., and Johnston, D. T. (2013). A basin Redox Transect at the Dawn of Animal Life. *Earth Planet. Sci. Lett.* 371-372, 143–155. doi:10.1016/j.epsl.2013.04.003

Sperling, E. A., Wolock, C. J., Morgan, A. S., Gill, B. C., Kunzmann, M., Halverson, G. P., et al. (2015). Statistical Analysis of Iron Geochemical Data Suggests Limited Late Proterozoic Oxygenation. *Nature* 523, 451–454. doi:10.1038/nature14589

Stolper, D. A., Love, G. D., Bates, S., Lyons, T. W., Young, E., Sessions, A. L., et al. (2017). Paleoecology and Paleoceanography of the Athel Silicilyte, Ediacaran-Cambrian Boundary, Sultanate of Oman. *Geobiology* 15, 401–426. doi:10.1111/gbi.12236

Stueeken, E. E., Zaloumis, J., Meixnerova, J., and Buick, R. (2017). Differential Metamorphic Effects on Nitrogen Isotopes in Kerogen Extracts and Bulk Rocks. *Geochimica et Cosmochimica Acta* 217, 80–94.

Thomazo, C., Ader, M., and Philippot, P. (2011). Extreme 15N-Enrichments in 2.72-Gyr-Old Sediments: Evidence for a Turning point in the Nitrogen Cycle. *Geobiology* 9, 107–120. doi:10.1111/j.1472-4669.2011.00271.x

van Gemenden, H., and Mas, J. (1995). in *Anoxygenic Photosynthetic Bacteria*. Editors R. E. Blankenship, M. T. Madigan, and C. Bauer (Springer), 49–85 .

van Maldegem, L. M., Sansjofre, P., Weijers, J. W. H., Wolkenstein, K., Strother, P. K., Wörmer, L., et al. (2019). Bisnorgammacerane Traces Predatory Pressure and the Persistent Rise of Algal Ecosystems after Snowball Earth. *Nat. Commun.* 10, 476. doi:10.1038/s41467-019-08306-x

Verne-Mismer, J., Ocampo, R., Callot, H. J., and Albrecht, P. (1986). Identification of a Novel C33 DPEP Petroporphyrin from Boscan Crude Oil : Evidence for Geochemical Reduction of Carboxylic Acids. *Tetrahedron Lett.* 27, 5257–5260. doi:10.1016/s0040-4039(00)85184-9

Vo, J., Inwood, W., Hayes, J. M., and Kustu, S. (2013). Mechanism for Nitrogen Isotope Fractionation during Ammonium Assimilation by Escherichia Coli K12. *Proc. Natl. Acad. Sci.* 110, 8696–8701. doi:10.1073/pnas.1216683110

Wang, D., Ling, H.-F., Struck, U., Zhu, X.-K., Zhu, M., He, T., et al. (2018a). Coupling of Ocean Redox and Animal Evolution during the Ediacaran-Cambrian Transition. *Nat. Commun.* 9, 2575. doi:10.1038/s41467-018-04980-5

Wang, W., Guan, C., Zhou, C., Peng, Y., Pratt, L. M., Chen, X., et al. (2017). Integrated Carbon, Sulfur, and Nitrogen Isotope Chemostratigraphy of the Ediacaran Lantian Formation in South China: Spatial Gradient, Ocean Redox Oscillation, and Fossil Distribution. *Geobiology* 15, 552–571. doi:10.1111/gbi.12226

Wang, X., Jiang, G., Shi, X., Peng, Y., and Morales, D. C. (2018b). Nitrogen Isotope Constraints on the Early Ediacaran Ocean Redox Structure. *Geochimica et Cosmochimica Acta* 240, 220–235. doi:10.1016/j.gca.2018.08.034

Werner, R. A., and Brand, W. A. (2001). Referencing Strategies and Techniques in Stable Isotope Ratio Analysis. *Rapid Commun. Mass. Spectrom.* 15, 501–519. doi:10.1002/rcm.258

Zhang, J., Fan, T., Zhang, Y., Lash, G. G., Li, Y., and Wu, Y. (2017). Heterogenous Oceanic Redox Conditions through the Ediacaran-Cambrian Boundary Limited the Metazoan Zonation. *Sci. Rep.* 7, 8550. doi:10.1038/s41598-017-07904-3

Zhang, X., Sigman, D. M., Morel, F. M. M., and Kraepiel, A. M. L. (2014). Nitrogen Isotope Fractionation by Alternative Nitrogenases and Past Ocean Anoxia. *Proc. Natl. Acad. Sci. USA* 111, 4782–4787. doi:10.1073/pnas.1402976111

Conflict of Interest: NS was employed by Vir Biotechnology, Inc.,

The remaining authors declare that the research was conducted in the absence of any commercial or financial relationships that could be construed as a potential conflict of interest